Consiglio Nazionale delle Ricerche
ISTITUTO DI ASTROFISICA SPAZIALE
E FISICA COSMICA

Active/passive shielding design scientific rationale for a future high energy telescope

Issue 3.0 – 20/10/2004
IASF/Bologna Internal Report n. 400/2004

Giuseppe Malaguti[1], Giovanni Pareschi[2], and Stefano Basso[2]

[1] IASF – Sezione di Bologna
[2] INAF-Merate

iASF
Sezione di Bologna
Area Ricerca di Bologna - Via Piero Gobetti, 101 - 40129 Bologna Italia
Tel. +39 051 6398688 - Fax +39 051 6398724
e-mail: iasf@bo.iasf.cnr.it - homepage http://www.bo.iasf.cnr.it
Cod. Fisc. 80054330586 - Part. IVA 02118311006

1. Introduction

The study of the universe in the 20-60 keV energy band is still hampered by the absence, up to now, of focusing telescopes for this energy band. The most sensitive experiment flown at these energies, BeppoSAX/PDS, had a flux limit of ≈200-300 μCrab. While INTEGRAL/IBIS, with unprecedented imaging capabilities for E>20 keV, has an angular resolution of 12 arcmin.

On the other hand, this region of the electromagnetic spectrum contains the potential for a dramatic improvement in our understanding of a number of key astrophysical problems which are still open, such as the origin of the cosmic X-ray background (CXB) in the 20-40 keV band where its energy density peaks, or the history of super-massive black hole (SMBH) growth (e.g.: Fiore et al. 2004).

Recent technological advancements in the field of both X-ray mirrors and CZT detectors allow for the first time the development of a moderate field of view (FOV), fine imaging, and deep sensitivity broad-band (≈0.5-70 keV) high-energy telescope. For E>20 keV, the key science driven performance requirements of such a mission are (Fiore et al. 2004):

a) high throughput (>400 cm^2) at 30 keV;
b) <15-20 arcsec HPD in a 15 arcmin FOV;
c) ≈0.4μCrab flux limit (1 Ms) in the 20-40 keV band;

The present report, starting from simulation data and experimental results, is aimed at the evaluation of the expected background and sensitivity for a future hard X-ray telescope in the 20-40 keV region as a function of various detector design trade-off parameters, i.e.: passive and active shield configurations, collimator aperture and height, detector dead area, etc.

2. Telescope sensitivity

The minimum detectable flux for a focusing optics based X-ray telescope is given by:

$$F_{\min} = n_\sigma \frac{\sqrt{B \cdot A_d}}{\varepsilon \cdot \eta \cdot (1-\gamma) \cdot A^i_{eff} \cdot \sqrt{N \cdot T \cdot \Delta E}} \quad photons \;\; cm^{-2} \; s^{-1} \; keV^{-1}, \qquad (1)$$

where B is the background flux (in counts cm^{-2} s^{-1} keV^{-1}), A_d is the spot area of each mirror module (cm^2), A^i_{eff} is the collection area of a single module weighted by the total mirror reflectivity (cm^2), N is the number of mirror modules, η is the fraction of incoming X-ray photons reflected within A_d, ε is the detector quantum efficiency, γ is the fraction of detector dead area (due to the pitch between two adjacent pixels, plus the possible vignetting caused by collimator walls), and n_σ is the statistical significance of the detection.

The value A_d depends upon the geometrical assembly of the telescope/detector and on the assumed fraction of focused photons, η. For $\eta = 0.5$, then A_d is given by the following relation:

$$A_d = \frac{\pi}{4}\left(\tan\left(HPD\right)\cdot FL\right)^2 \quad cm^2, \tag{2}$$

where *HPD* is the Half Power Diameter angular resolution, and *FL* the focal length in cm.
On the other hand, the effective area, A_{eff}, of a X-ray mirror telescope, based on Wolter I optics, is approximately given by:

$$A_{eff} \propto (1-\xi)\cdot FL^2 \cdot \alpha_c^2 \cdot R^2 \quad cm^2, \tag{3}$$

where α_c is the reflection critical (i.e. maximum) angle, *R* is the reflectivity of the mirrors, and ξ is the telescope area loss due to the vignetting caused by the spider arms and thickness of the mirror shell walls. Equation (3) clearly shows that the value of A_{eff} can be increased either by having a large focal length, and/or by using multi-layer mirrors which allow a higher upper threshold value for α_c.

3. Background estimates and collimator aperture

The background of high energy telescopes can be divided in two main components:

i. Hadron induced:
  a. Cosmic ray induced (prompt and delayed);
  b. Radiation belts;
  c. Solar activity;

ii. Photon induced:
  a. CXB;
  b. Atmospheric albedo;

Figure 1 shows the expected background on Constellation-X/HXT simulated for the same detector design both for the LEO and L2 orbit scenario (Armstrong et al. 1999). The hadronic induced component is indicated as “activation” and the difference between the contributions from radioactive isotopes created in BGO and CZT is specifically indicated.
While a detailed background rate spectrum evaluation requires a dedicated MonteCarlo simulation of the telescope/spacecraft based on photon/particle transport codes (e.g.: GEANT), some preliminary assessment is possible by scaling from experimental data (solid state detectors, CZT based, flown aboard stratospheric balloons or satellite borne telescopes working in the same energy range) and/or from simulations results available from other missions.

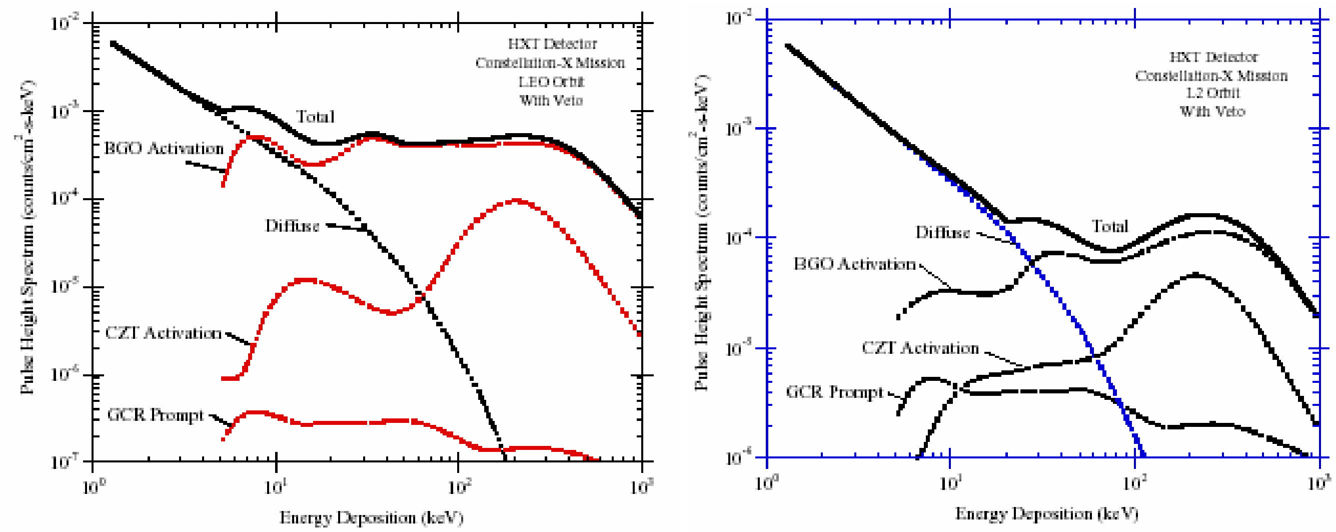

Figure 1: GEANT based Monte-Carlo simulation results of the background flux spectrum components expected for the hard X-ray telescope on-board the Constellation-X mission. The expected background spectra are shown for an LEO (left panel) and L2 (right panel) scenario (from Armstrong et al. 1999).

Recent balloon experiments (Bloser et al. 2002) based on an actively (organic plus inorganic) and passively shielded CZT detector have measured a background level of ~3×10^{-3} cts cm^{-2} s^{-1} keV^{-1} in the 20-40 keV region for a detector with a 40°×40° aperture (zero response FOV). Assuming a factor ~3 reduction due to residual (≈3 g cm^{-2}) atmospheric absorption, this value is equivalent to ~9×10^{-3} cts cm^{-2} s^{-1} keV^{-1} in a satellite environment, that, for a collimator aperture of 3°×3°, is equivalent to ~5×10^{-5} cts cm^{-2} s^{-1} keV^{-1}.

On the other hand, the cosmic diffuse background at E>20 keV is approximately (Zombeck, pag 197): $B(E)=167\times E^{-2.38}$ photons cm^{-2} s^{-1} keV^{-1} sr^{-1}. This would imply a collimator aperture just below ~2°×2° to reach the level of ~5×10^{-5} cts cm^{-2} s^{-1} keV^{-1}. The required field of view in this case is only marginally smaller than what obtained by scaling from balloon measurements. This slight disagreement can be ascribed to the very large field of view used for the balloon measurement (≈1600 square degrees) which implies significant errors when extrapolating down to narrow fields.
The Constellation-X/HXT simulation results shown in figure 1 give indications on how the in-flight background can vary depending on the orbit choice. For the simulated detector set-up in fact, the total background expected at ≈30 keV in L2 is about 4 times less than what expected in LEO. More in particular, the photon diffuse component contributes for ≈20% of the total expected background for a LEO medium inclination orbit, while this fraction goes up to ≈50% for a L2 scenario. The remaining background fraction is dominated by BGO activation, with a small contribution caused by CZT activation. This is probably due to the fact that, for these simulations, the Con-X/HXT configuration used was optimized for L2 and not for LEO (the adopted thickness of the BGO shield was 1.9 cm, or 13.5 g cm^{-2}). This high volume of BGO has translated into an overshielding against the direct hadronic component, causing a high BGO radioactive isotope activation contribution. This clearly indicates that the final BGO thickness, and detector geometry/configuration in general, will have to be chosen (i.e. optimized) also on the basis of the selected orbit scenario.

iASF
Sezione di Bologna
Area Ricerca di Bologna - Via Piero Gobetti, 101 - 40129 Bologna Italia
Tel. +39 051 6398688 - Fax +39 051 6398724
e-mail: iasf@bo.iasf.cnr.it - homepage http://www.bo.iasf.cnr.it
Cod. Fisc. 80054330586 - Part. IVA 02118311006

For the project under study, moreover, the expected background component due to BGO activation can be expected to be significantly lower than in the Con-X/HXT case, for two reasons:

a) the upper energy threshold will be lower, i.e. ~80-100 keV so that an active/passive shielding system based upon plastic (or inorganic scintillator with a thickness significantly smaller than what used for detectors operating in the hundreds of keV region) coupled with a graded collimator can be feasible;
b) in the case of a low equatorial orbit (HEXIT-Sat scenario, ~600 km, few degree inclination) or very high circular orbit (Simbol-X present option) the contribution from particle background will be further decreased.

The detector PDS (Phoswich Detector System) onboard the BeppoSAX satellite based on NaI-CsI phoswich with passive (≈1.3°) and active (CsI+plastic) shields, has measured a background level which, scaled to a 1 mm detector thickness, is equal to 5×10^{-5} cts cm^{-2} s^{-1} keV^{-1}. As suggested by Fiore et al. (2004), this value can be used as a reference for the hadronic component, to which one has to sum the contribution of the CXB component to get the total expected background.

The summary of background evaluations is given in Figure 2, that shows the minimum (referring to balloon data) and maximum (from the measured cosmic X-ray diffuse background covolved to the collimator angular response, and summed to the particle background component measured by BeppoSAX/PDS) estimates for the background as a function of collimator zero response aperture. The continuous (red and blue) lines refer to a setup in which the detector opening angle is further limited (by about 2 deg^2) by the angular obscuration provided by the structure of the optics structure itself plus the possible introduction of 'wings' opaque to hard X-rays placed around it (see figure 4).

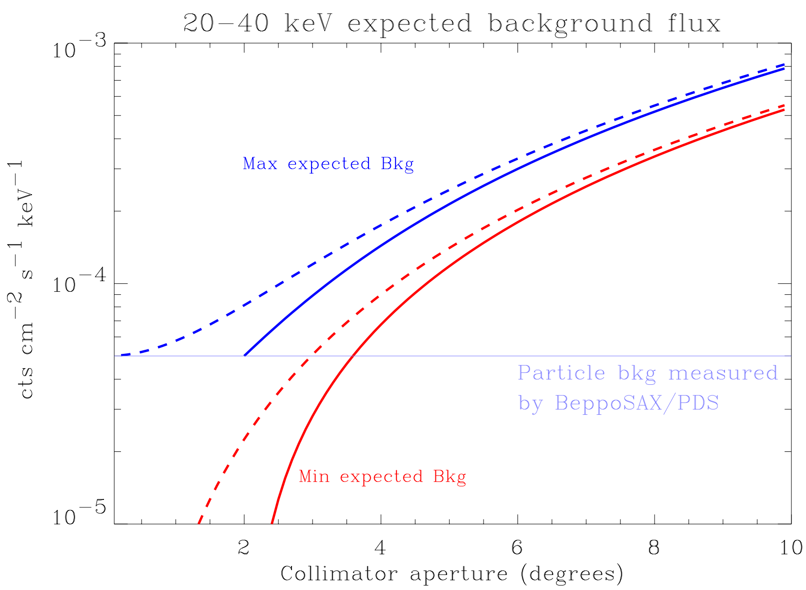

Figure 2: Expected background flux in the 20-40 keV band as a function of the collimator aperture. The blue (maximum expected value) and red (minimum expected value) profiles, indicate the expected count rate expected in a configuration with (continuous line) and without (dashed lines) the contribution offered by 'wings' around the optics, respectively.

4. Sensitivity evaluation

Using equation (1) and assuming the expected background levels shown in figure 2, it is possible to evaluate the minimum detection sensitivity for various telescope configurations. In the present feasibility phase study we have taken into considerations three mission scenarios, the key parameters of which are listed in table 1.

Table 1: Key telescope parameters assumed for the evaluation of the sensitivity in the various envisaged mission scenarios.

Mission scenario	HP (arcsec)	FL (m)	A_{eff} (cm^2)
HEXIT-Sat (4 modules):	15	8	500
Simbol-X:	30	30	600
Simbol-X-plus[(a)]	15	30	600

[(a)]We have indicated as "Simbol-X-plus" a mission with the same characteristics as the present Simbol-X configuration, but with the angular resolution in terms of HPD improved of a factor 2.

For each configuration, we have assumed a 50% encircled diameter, 95% detector quantum efficiency, and a 1 Ms integration time. The resulting expected 3σ minimum detection sensitivity in the 20-40 keV energy band for three different background levels, is shown in Figure 3 as a function of the detector active area loss (factor $(1-\gamma)$ shown in equation (1)). In the current proposed configurations, the value of γ is dominated by two factors:

a) the detection area loss due to the finite active pixel pitch in the detector matrices;
b) the dead area caused by the collimator wall thickness, the importance of which can vary for the different passive shielding configurations (see section 5).

Figure 3 indicates that, in the HEXIT-Sat scenario, an active area loss γ of $\approx 8\div 10\%$ and up to >15% can still allow to meet the 0.35 μCrab (1 Ms integration time) requirement (Fiore et al. 2004) in the case of 1×10^{-4} and 5×10^{-5} cts cm^{-2} s^{-1} keV^{-1} background total (hadronic + CXB component) level, respectively.

It is important to remind that the sensitivity evaluations shown in figure 3 refer to the key telescope configuration parameters indicated in table 1, which are, in this phase, not frozen.
In the case of HEXIT-Sat, for instance, an increase of FL up to 10 m, would give an improvement in sensitivity (see equations (1) and (3)) of $\Delta S \propto \frac{\sqrt{A_d}}{A_{eff}} = \frac{FL}{FL^2} = 20\%$.

In the Simbol-X case, on the other hand, the focal length is fixed (being one of the boundary conditions of the flight), but the value of A_{eff} can be increased by introducing multi-layer based external shells which would allow a larger value for α_c (from 8.5′ to 10.8′), which can, conservatively, allow an increase in A_{eff}, and therefore in sensitivity, by ≈30%.

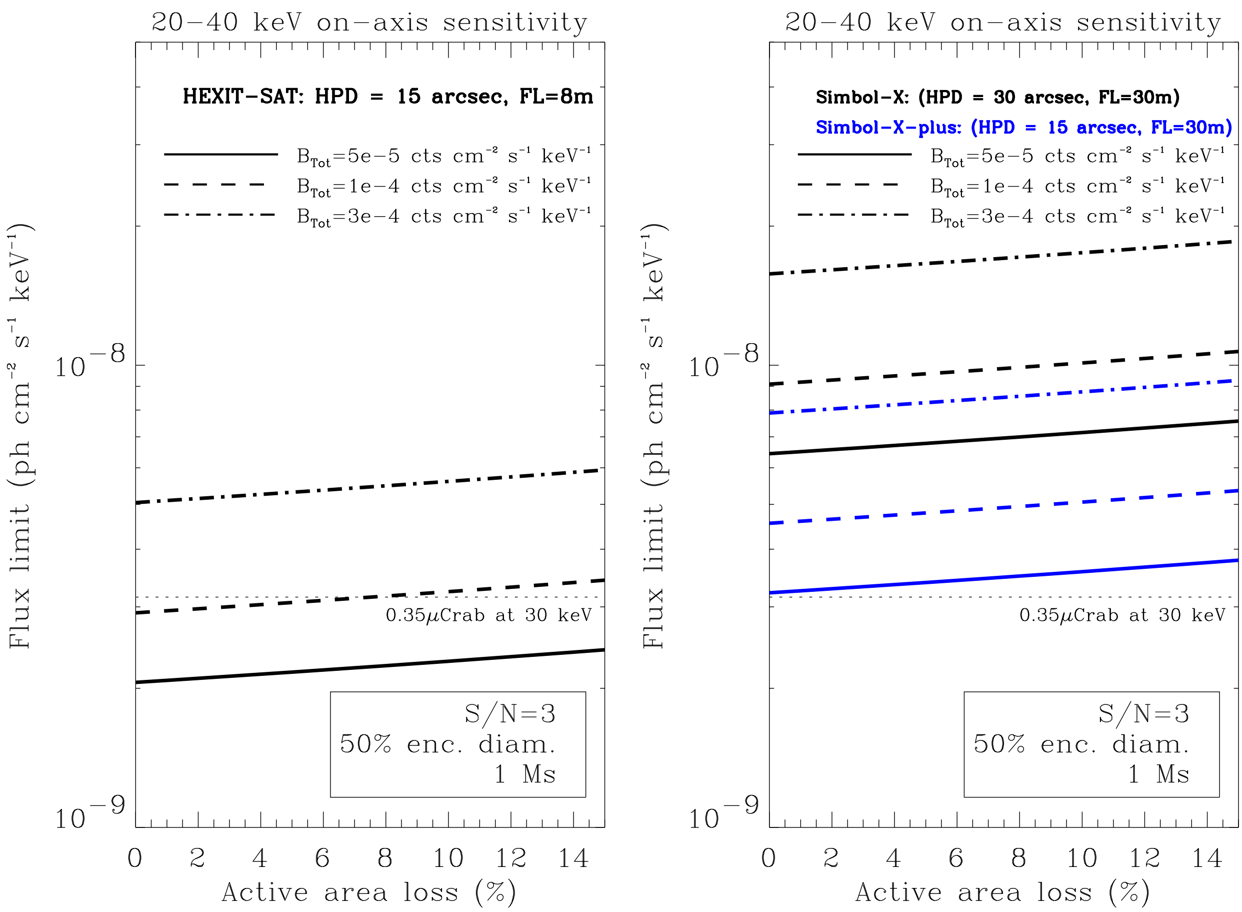

Figure 3: Expected 20-40 keV minimum detection sensitivity for three mission scenarios (see text) and different background levels, as a function of the detector active area loss. The superimposed horizontal dotted line indicates the scientific requirements of 0.35μCrab at 30 keV from Fiore et al. (2004).

5. Passive shielding design requirements vs active area loss

The scientific requirement of having a narrow field of view for the focal plane detector opens a number of possible configuration designs, which have been addressed in the Alenia-LABEN report "Preliminary T/S designs of the focal plane" (TL 20671). The technical approach can be divided into two separate solutions (see figure 4):

a) Tube-shaped passive and active shields, with a higher, graded, high-Z collimator that defines the zero angle field of view of the detector;
b) Short tube-shaped passive and active shields, coupled with two concentric and coplanar graded, high-Z, discs placed at different heights above the detector, that define its zero angle field of view.

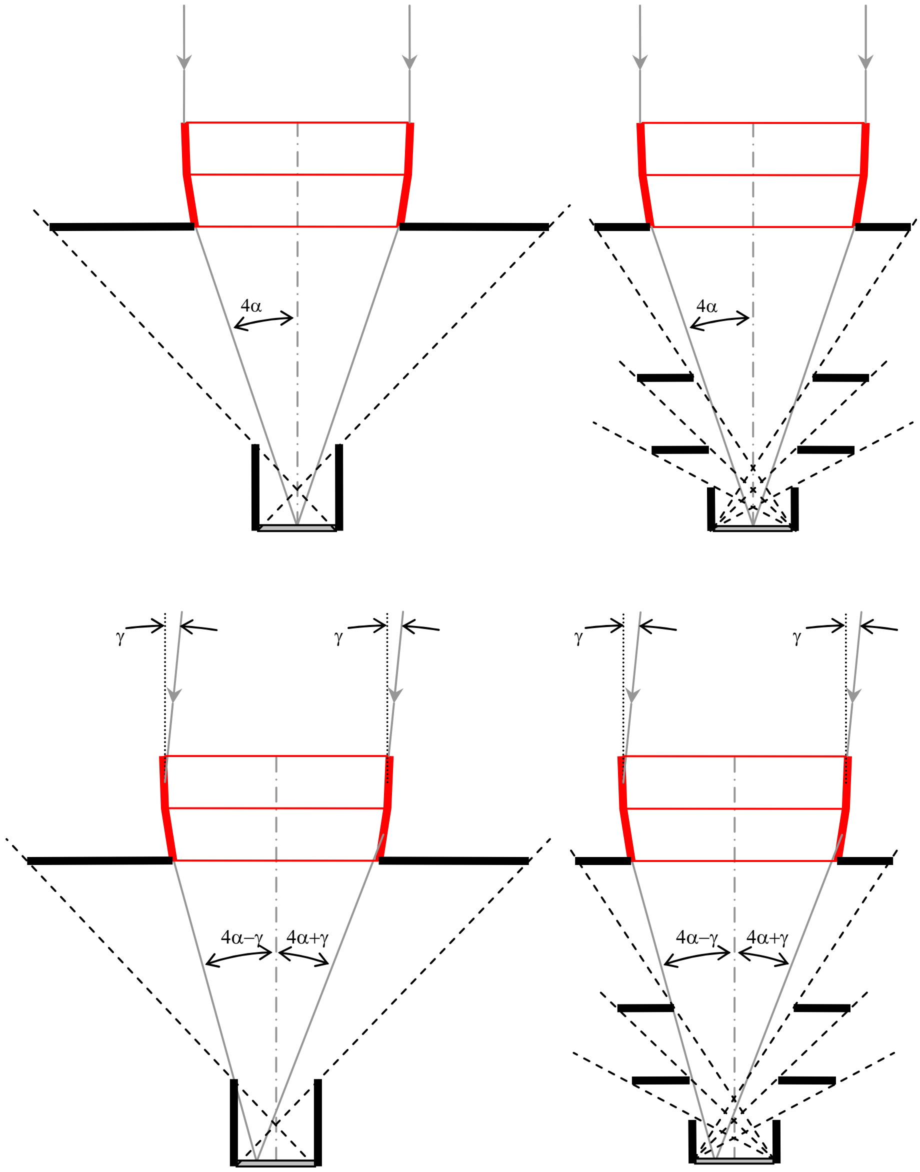

The four diagrams shown in figure 4 indicate an example of the various possible collimating configurations, which refer to option (a) and (b). The arrows represent the incoming X-ray photons, which are reflected by the mirror assembly (shown in red). The lateral wings adjacent to the optics structure represent the further passive shielding mentioned in section 3, and in point (d) of the conclusions. The incoming X-ray photons are focused on the detection plane with an incident angle equal to $4\alpha \pm \gamma$, where α is the reflection angle and γ is the off-axis inclination of the primary X-ray.

Figure 4:
Top left:
Collimator tube in the case of on-axis incident photons;
Top-right:
Two-disc collimation assembly for on-axis incident photons;
Bottom-left:
Tube for on-axis;
Bottom right:
Two-disc for off-axis.

The general concept of options (a) and (b) indicated above and exemplified in figure 4, are of course valid for any satellite-borne high energy telescope operating in the tens of keV region. The shielding the detector(s) against the background caused by CXB photons is particularly important for the formation flight concept, proposed for the Simbol-X (Ferrando et al. 2003) and XEUS (Parmar et al. 2003) mission projects. In this configuration in fact, the two spacecraft scenario prevents the use of a single cell telescope baffle as a passive shield against the unwanted photons.

Solution (a), shown in the left panels of figure 4, requires a high number of “tubes” in order to maintain an acceptable (i.e.: technically feasible) height for the collimator walls (up to one collimator for each of the 37 crystals, see the Alenia-LABEN document for details). Solution (b), on the other hand, is directly feasible for HEXIT-Sat, by means of an expandable optical bench, while it needs a firm feasibility assessment for the Simbol-X scenario. Moreover, for solution (b), the basic dimension parameters (lower collimator height, disc 1 and 2 position, radii, and thickness) allow a number of valid technical solutions, the trade-offs of which are currently under study.

In the case of solution (a), the "multi-tube" design implies a possible increase of the dead area due to the collimator wall thickness (≈500μm). The expected sensitivity profiles shown in figure 3 indicate that the trade-off between dead area loss and collimator wall height must be analyzed in detail before freezing the detection assembly configuration design. On the other hand, the effect of active area loss can be counterbalanced with a parallel increase of effective area attainable with the introduction of multi-layer mirrors.

6. Design requirements and conclusions

The above results give first indications concerning the critical areas which must be addressed in a feasibility study and design concept development of the active and passive shielding for a future hard X-ray telescope mission. The key points can be summarized as follows:

a) **Collimator aperture limit:** Given the 0.35 μCrab (at 20-40 keV in 1 Ms) requirement on the minimum detectable flux, and the present uncertainties on the final telescope design, it is not possible to freeze in this phase the aperture of the detector (active and passive) shielding system. The current constraints given by the telescope field of view and focal length, imply a detection plane aperture angle between 1.5 and 3 degrees (see Figure 2). The impact of such a collimator needs to be investigated in terms of the overall structure design.

b) **Active area loss:** Two are the parameters that can cause significant active area loss: detection plane dead area due to finite pixel pitch, and vignetting caused by the passive shield collimating system. The first factor needs to be minimized by limiting the loss of photons interacting in the separation zones between two pixels. As far as vignetting is concerned, it is important to point out that, this depends on the X-ray interaction in the detection plane and that, in any case, on-axis photon are not affected by this factor in all the envisaged collimator designs (mono-cell tube, multi-cell tube, and two disc configuration). However, the multi-cell configuration, which allows shorter collimator walls, can determine an active area loss distributed over the entire telescope field of view. The possible trade-offs between all the configuration will have to be studied in details.

c) **Two disc solution:** The technical implementation of the two-disc solution also for the Simbol-X scenario must be firmly assessed in order to avoid the expected area loss for a multi-cell collimator.

d) **Optics baffle:** The possibility to place a "wing" system around the structure containing the optics can result in a further diffuse background reduction. The effect of this further shielding can depend upon the final telescope configurations and needs to be precisely evaluated for both options, HEXIT-Sat and Simbol-X.

e) **Plastic around the graded shield:** It is also important to remind that the background evaluation shown in Figure 2 has been scaled from a balloon experiment for which the CZT detector was actively and passively shielded. The passive shielding was done by means of a graded (Pb-Sn-Cu) collimator. The active shielding included a BGO crystal on the rear of the detection plane, plus a plastic detector surrounding the passive collimator to reject local photon production. The development of the design of a future hard X-ray satellite telescope must therefore foresee an analogous combination of active (possibly with either a thinner BGO, or with inorganic crystal replaced by plastic to decrease the activation component at low energies) and passive (graded) shielding;

f) **HEXIT-Sat vs SIMBOL-X scenario:** All the above considerations and factors can have different impacts depending on the final overall telescope design. It is therefore important, in this preliminary design phase, to assess the feasibility and evaluate the scientific performance of both scenarios.

Acknowledgements:

We thank Fabrizio Fiore for very helpful inputs and discussions.

References:

1. Alenia-LABEN report "*Preliminary T/S designs of the focal plane*" (TL 20671)
2. Armstrong, T.W., et al. 1999, "*Initial estimates of radiation backgrounds for the hard- X-ray telescope (HXT) on the planned Constellation-X mission*", Report No. SAIC-TN-99015R3;
3. Bloser, P.F., et al. 2002, "*Balloon flight background measurement with actively-shielded planar and imaging CZT detectors*", Proc. SPIE Vol. 4497, p. 88-99, X-Ray and Gamma-Ray Instrumentation for Astronomy XII, Kathryn A. Flanagan; Oswald H. Siegmund; Eds.;
4. Ferrando, P. 2003, "*SIMBOL-X: a new-generation hard x-ray telescope*", Optics for EUV, X-Ray, and Gamma-Ray Astronomy. Edited by Citterio, Oberto; O'Dell, Stephen L. Proceedings of the SPIE, Volume 5168, pp. 65-76;
5. Fiore, F. et al. 2004, "*HEXIT-Sat: a mission concept for X-ray grazing incidence telescopes from 0.5 to 70 keV*", SPIE Proc., in press, astro-ph/0407647;
6. Parmar, A., et al. 2003, "*XEUS: the X-ray evolving universe spectroscopy mission*", X-Ray and Gamma-Ray Telescopes and Instruments for Astronomy. Edited by Joachim E. Truemper, Harvey D. Tananbaum. Proceedings of the SPIE, Volume 4851, pp. 304-313;
7. Zombeck, M.V., "*Handbook of space astronomy and astrophysics*", Cambridge: University Press, 1990, 2nd ed.;

Area Ricerca di Bologna - Via Piero Gobetti, 101 - 40129 Bologna Italia
Tel. +39 051 6398688 - Fax +39 051 6398724
e-mail: iasf@bo.iasf.cnr.it - homepage http://www.bo.iasf.cnr.it
Cod. Fisc. 80054330586 - Part. IVA 02118311006